

Atomic motion in light beams possessing orbital angular momentum

W. L. Power

Optics Section, Blackett Laboratory, Imperial College, London SW7 2BZ, United Kingdom

L. Allen, M. Babiker, and V. E. Lembessis

Department of Physics, University of Essex, Colchester CO4 3SQ, United Kingdom

(Received 22 November 1994)

A theory is developed that leads to the description of the internal and gross motions of an atom interacting with an arbitrary light field. The general results are then applied to the case of a Laguerre-Gaussian (LG) mode, one of a class of modes of electromagnetic radiation that possess orbital angular momentum. A number of effects are predicted, notably, an azimuthal shift in the atomic resonance, a modified radiation pressure force, and an associated torque on the atom. It is pointed out that the effects originate in the processes of the transfer of linear and orbital angular momentum from the field to the atomic gross motion. The strengths of the effects are assessed in relation to the normal axial Doppler shift and the linear light pressure force. The motion of atoms and ions subject to the LG pressure force is studied by solving the classical equation of motion. Trajectories clearly exhibiting the effects of orbital angular momentum are displayed for a free atom and for an ion in a two-dimensional trap and in a Paul trap.

PACS number(s): 42.50.Vk, 32.80.Pj

I. INTRODUCTION

It has long been known that light exhibits interesting and potentially exploitable radiation pressure effects that are associated with its energy-momentum properties [1,2]. In fact, since the basic mechanisms were first reconsidered [3], light pressure phenomena have been under intensive study by both theory and experiment [4]. It is only relatively recently, however, that many of the effects involving radiation pressure on the gross motion of atoms have been observed [5].

Most theoretical treatments of radiation pressure effects on atoms have used a plane-wave approximation of the light; any light field can, in principle, be decomposed into a superposition of plane waves. However, in some situations, such as the case we consider here, this decomposition can be very complicated and can obscure interesting effects. In the theoretical development we discuss, we need only assume that the light belongs to a well-defined mode of the radiation field. Thus the detailed form of the mode is left general until the results of the theory are applied to the specific case of interest.

Recent advances in the theory of nonuniform light have demonstrated that light beams can possess orbital angular momentum and that this angular momentum should be transferrable to material objects interacting with them [6]. This orbital angular momentum is distinct from the spin angular momentum associated with circularly polarized light and can occur in modes that are linearly polarized. The orbital angular-momentum equivalent of Beth's famous experiment [7], which used circularly polarized light to rotate a birefringent plate and so transfer angular momentum from a light beam to a macroscopic material, is in progress [8].

The purpose of this paper is to present a theory for the

motion of a two-level atom in an arbitrary light field and apply the general results obtained to the case where the light field in question is a Laguerre-Gaussian mode. Laguerre-Gaussian modes belong to a class of readily producible laser modes characterized by their orbital angular-momentum properties. In addition to the interaction with such modes the motion of the atom is also subject to spontaneous emission effects that occur due to the interaction with an infinite reservoir of vacuum modes. Spontaneous emission effects are not taken into account *ab initio* in our treatment, but can be included later using some simple and straightforward arguments. The procedure will lead to results that can be widely applied.

The paper is organized as follows. In Sec. II we define the Hamiltonian of the system and demonstrate how it can be used to determine the time evolution of variables pertaining to the light and of the internal and gross motions of the atom. The procedure yields general expressions for the reactive and dissipative forces on the atom for an arbitrary field distribution, which are then shown to produce the well-known results characteristic of a linearly polarized plane wave in the appropriate limit. In Sec. III the theory is applied to the case of a two-level atom interacting with a Laguerre-Gaussian (LG) mode. Here significant results relating to the shift of the atomic resonance and to a torque on the atom are presented and compared with the predictions for the same atom interacting with a plane wave [9,10]. In Sec. IV we consider the numerical solution of the equation of motion for atoms and ions under the influence of the LG radiation forces. We show how this leads transparently to the presentation of atomic trajectories in a number of experimentally viable contexts. In particular we present trajectories for a free atom, an ion in a two-dimensional poten-

tial well, and finally an ion in a Paul trap. Section V contains our comments and final conclusions.

II. THEORY

Our model is defined as a two-level atom or ion, henceforth referred to as the atom, interacting with light whose frequency is denoted ω but whose spatial distribution is initially unspecified. The atomic excitation frequency is denoted by ω_0 and the atom is assumed to be interacting with the light via its dipole moment vector \mathbf{d} . The atom may be subject further to a trapping potential $U(\mathbf{R})$, which acts to confine its motion in one, two, or all three dimensions. The Hamiltonian operator appropriate for this model is written as

$$H = \frac{\mathbf{P}^2}{2M} + U(\mathbf{R}) + \hbar\omega_0\pi^\dagger\pi + \hbar\omega a^\dagger a - \mathbf{d} \cdot \mathbf{E}(\mathbf{R}). \quad (1)$$

Here \mathbf{P} and \mathbf{R} are the momentum and the position vectors of the atomic center of mass. The operators π and π^\dagger and a and a^\dagger are, respectively, the lowering and the raising operators for the atom and the light. The Hamiltonian (1) is correct only to leading order in the interaction (electric-dipole approximation) between the light and the atom and we have dropped all zero-point energies. Other convection-type effects, such as those arising from the motion of the electric dipole in the laser field, are considered small and therefore not included. For example, we ignore the Röntgen interaction [11,12], and this has the simple consequence that the canonical and the mechanical momentum of the center of mass are identical [13]. The quantized electric-field operator $\mathbf{E}(\mathbf{R})$ can be expressed in terms of a general normalized mode function $\mathcal{E}(\mathbf{R})$ as

$$\mathbf{E}(\mathbf{R}) = i \{ a \mathcal{E}(\mathbf{R}) - \mathcal{E}^*(\mathbf{R}) a^\dagger \}. \quad (2)$$

It is convenient to express \mathcal{E} in terms of a real amplitude function $\epsilon(\mathbf{R})$ and a phase factor involving a real function $\Theta(\mathbf{R})$. Thus we set

$$\mathcal{E} = \epsilon(\mathbf{R}) e^{i\Theta(\mathbf{R})}. \quad (3)$$

We also represent the dipole operator by the familiar expression

$$\mathbf{d} = \mathbf{D}_{12}(\pi + \pi^\dagger), \quad (4)$$

where \mathbf{D}_{12} is the dipole matrix element between levels 1 and 2. We can then write the electric-dipole term in the Hamiltonian in the form

$$\mathbf{d} \cdot \mathbf{E} = i\hbar \{ \pi^\dagger a f(\mathbf{R}) - f^*(\mathbf{R}) a^\dagger \pi \}, \quad (5)$$

where

$$f(\mathbf{R}) = G(\mathbf{R}) e^{i\Theta(\mathbf{R})} \quad (6)$$

with $G(\mathbf{R})$ given by

$$G(\mathbf{R}) = \frac{1}{\hbar} \mathbf{D}_{12} \cdot \epsilon(\mathbf{R}). \quad (7)$$

For a plane wave G corresponds to the Rabi frequency Ω and is real for linearly polarized light. In the present case, where ϵ is the amplitude for an arbitrary field distribu-

tion, G corresponds to a position-dependent Rabi frequency. It is convenient to express the interaction in terms of G and Θ rather than f . The Hamiltonian (1) now becomes

$$H = \frac{\mathbf{P}^2}{2M} + U(\mathbf{R}) + \hbar\omega_0\pi^\dagger\pi + \hbar\omega a^\dagger a - i\hbar \{ \pi^\dagger a G(\mathbf{R}) e^{i\Theta(\mathbf{R})} - G(\mathbf{R}) e^{-i\Theta(\mathbf{R})} a^\dagger \pi \}. \quad (8)$$

The time evolution of the system is derivable from the Heisenberg equation of motion. For an operator O this is

$$\frac{dO}{dt} = \frac{1}{i\hbar} [O, H], \quad (9)$$

which can be formally integrated to give

$$O(t) = O(0) + \frac{1}{i\hbar} \int_0^t [O(t'), H(t')] dt', \quad (10)$$

where $O(0)$ denotes the initial value of O .

The linear momentum associated with the atomic gross motion is the dynamical property of the system whose evolution with time is initially of relevance. Evaluating the commutator in Eq. (9) for \mathbf{P} using Eq. (8) we obtain

$$\begin{aligned} \mathbf{P}(t) = & \mathbf{P}(0) - \int_0^t \nabla U(\mathbf{R}) dt' \\ & + i\hbar \int_0^t dt' \{ \pi^\dagger(t') a(t') \nabla [G(\mathbf{R}, t') e^{i\Theta(\mathbf{R}, t')}] \\ & - \nabla [e^{-i\Theta(\mathbf{R}, t')} G(\mathbf{R}, t')] a^\dagger(t') \pi(t') \}. \end{aligned} \quad (11)$$

In order to derive the time evolution of the momentum from this result, we need to determine the explicit dependence of the operators within the integral sign of the last term of Eq. (11) followed by a direct evaluation of the time integral. We seek expressions that are valid up to second order in the coupling, which amounts to evaluating terms to order $|G|^2$. We consider first the time evolution of the operators within the integral sign in the last term of Eq. (11).

The evolution of each of the atomic and field operators is also based on the Heisenberg equation of motion. For the atomic lowering operator we obtain

$$\begin{aligned} \pi(t) = & e^{-i\omega_0 t} \left[\pi(0) + \int_0^t dt' e^{i\omega_0 t'} \{ 2\pi^\dagger(t') \pi(t') - 1 \} \right. \\ & \left. \times a(t') G(\mathbf{R}, t') e^{i\Theta(\mathbf{R}, t')} \right]. \end{aligned} \quad (12)$$

The evolution of the field annihilation operator a turns out to be in the form

$$a(t) = e^{-i\omega t} \left[a(0) + \int_0^t dt' e^{i\omega t'} G(\mathbf{R}, t') e^{-i\Theta(\mathbf{R}, t')} \pi(t') \right]. \quad (13)$$

Expressions for the raising operators are obtainable as simply the Hermitian conjugates of Eqs. (12) and (13).

Finally, we need the time evolution of the amplitude $G(\mathbf{R}, t)$ and the phase $\Theta(\mathbf{R}, t)$ characterizing the interaction. We confine ourselves to the leading order in the interaction while making use of the Heisenberg equation of motion (9). We find

$$G(\mathbf{R}, t) = G(\mathbf{R}_0) + \frac{\nabla G(\mathbf{R}_0) \cdot \mathbf{P}}{M} t \quad (14)$$

and

$$e^{i\Theta(\mathbf{R}, t)} = e^{i\Theta(\mathbf{R}_0)} e^{i\delta t}, \quad (15)$$

where δ is given by

$$\delta = \frac{1}{2M} (\mathbf{P} \cdot \nabla \Theta + \nabla \Theta \cdot \mathbf{P})_0. \quad (16)$$

Throughout, the label zero denotes operators at the initial time $t=0$. The second term in Eq. (14) has a direct interpretation; it describes the effects of the change in amplitude with position while, as we argue below, the term involving δ represents a Doppler shift in the resonance frequency.

We use the notation

$$\langle \mathbf{P}(t) \rangle = \langle \Psi | \mathbf{P}(t) | \Psi \rangle \quad (17)$$

to denote the expectation value of the momentum operator in a well-defined state $|\Psi\rangle$ of the system, at time t . The state $|\Psi\rangle$ need only be characterized by the initial average photon number n_k of the mode and occupation number n_2 of the upper atomic level 2

$$n_k = \langle \Psi | a^\dagger(0) a(0) | \Psi \rangle, \quad n_2 = \langle \Psi | \pi^\dagger(0) \pi(0) | \Psi \rangle. \quad (18)$$

The occupation number n_1 of the lower state of the two-level system is determined trivially from the normalization condition $n_1 + n_2 = 1$.

The evaluation of $\langle \mathbf{P}(t) \rangle$ now follows straightforwardly, albeit laboriously, by direct use of Eq. (11), making use of Eqs. (12)–(15). Throughout the calculation we retain terms only up to second order in the coupling, that is, second order in G_0 . We find after much algebra

$$\begin{aligned} \langle \mathbf{P}(t) \rangle = & \mathbf{P}(0) - \int_0^t \nabla U(\mathbf{R}) dt' \\ & + i\hbar [n_k(2n_2 - 1) + n_2] \\ & \times \{ G_0 \nabla G_0 I_1(t) + i \nabla \Theta_0 G_0^2 I_2(t) \}. \end{aligned} \quad (19)$$

For ease of notation we shall drop the label zero in all subsequent expressions of this section so that, unless otherwise stated, the functions G and Θ refer to those evaluated initially. The time dependence in the last term is contained entirely in the functions $I_1(t)$ and $I_2(t)$, which are given explicitly by

$$I_1(t) = 4i \int_0^t \frac{\sin^2 \left[\frac{\Delta t'}{2} \right]}{\Delta} dt' \quad (20)$$

and

$$I_2(t) = 2 \int_0^t \frac{\sin(\Delta t')}{\Delta} dt', \quad (21)$$

where Δ is the effective detuning

$$\Delta = \omega - \omega_0 - \delta \quad (22)$$

with δ given by Eq. (16).

The average force on the atom $\langle \mathbf{F} \rangle$ associated with the

atomic momentum $\langle \mathbf{P} \rangle$ is formally obtainable by direct use of the Heisenberg equation

$$\mathbf{F}(t) = \frac{d\mathbf{P}}{dt} = \frac{1}{i\hbar} [\mathbf{P}, H]. \quad (23)$$

The same procedure leading to Eq. (19) may be used to derive the average force. We have verified by explicit calculation that the results thus obtained coincide with the classical assignment

$$\langle \mathbf{F}(t) \rangle = \frac{d}{dt} \langle \mathbf{P}(t) \rangle \quad (24)$$

so that the average force can be found simply by differentiating the right-hand side of Eq. (19). This yields a force that can be written naturally as a sum of three components, namely, the confining force $-\nabla U$ plus two radiation pressure forces. These forces will be identified as a reactive force and a dissipative one

$$\langle \mathbf{F} \rangle = -\nabla U(\mathbf{R}) + \langle \mathbf{F} \rangle_{\text{react}} + \langle \mathbf{F} \rangle_{\text{dissip}}. \quad (25)$$

The first (reactive) force is given by

$$\begin{aligned} \langle \mathbf{F} \rangle_{\text{react}} = & -4\hbar [n_k(2n_2 - 1) + n_2] \\ & \times G(\mathbf{R}) \nabla G(\mathbf{R}) \frac{\sin^2 \left[\frac{\Delta t}{2} \right]}{\Delta} \end{aligned} \quad (26)$$

and the second (dissipative) force by

$$\begin{aligned} \langle \mathbf{F} \rangle_{\text{dissip}} = & -2\hbar [n_k(2n_2 - 1) + n_2] \\ & \times G^2(\mathbf{R}) \nabla \Theta(\mathbf{R}) \frac{\sin(\Delta t)}{\Delta}. \end{aligned} \quad (27)$$

The reason for the emphasis on the dissipative nature of the force will shortly become clear.

The formalism has so far dealt with the interaction of the atom with only one radiation mode and account needs to be taken of the effects of spontaneous emission from the excited state to the ground state. This can be introduced from the outset, as we plan to show in a forthcoming paper [14], but in order not to obscure the main thrust of the argument here, we have chosen to simplify the treatment. As we now show, we can use arguments leading to equally valid results. Denoting the decay rate of the excited state by Γ , we define the availability of the excited state as the survival rate dp/dt at time t by [15]

$$\frac{dp}{dt} = \Gamma e^{-\Gamma t}. \quad (28)$$

As the force is due to transition from the excited state the time averaged force is

$$\begin{aligned} \langle \bar{\mathbf{F}} \rangle = & \int dp \langle \mathbf{F} \rangle \\ = & \int_0^\infty \left[\frac{dp}{dt} \right] \langle \mathbf{F} \rangle dt \\ = & \int_0^\infty \langle \mathbf{F} \rangle \Gamma e^{-\Gamma t} dt. \end{aligned} \quad (29)$$

On substituting from Eqs. (26) and (27), we find that we only need to evaluate standard integrals and we are led to

write, for the time-averaged reactive force,

$$\begin{aligned} \langle \bar{\mathbf{F}} \rangle_{\text{react}} &= -4\hbar[n_k(2n_2-1)+n_2]G(\mathbf{R})\nabla G(\mathbf{R})\Gamma \\ &\times \int_0^\infty dt e^{-\Gamma t} \frac{\sin^2\left(\frac{\Delta t}{2}\right)}{\Delta} \\ &= -4\hbar[n_k(2n_2-1)+n_2]G(\mathbf{R})\nabla G(\mathbf{R}) \\ &\times \frac{1}{2} \left[\frac{\Delta}{\Delta^2+\Gamma^2} \right]. \end{aligned} \quad (30)$$

Similarly, we find for the time-averaged dissipative force,

$$\begin{aligned} \langle \bar{\mathbf{F}} \rangle_{\text{dissip}} &= -4\hbar[n_k(2n_2-1)+n_2]G^2(\mathbf{R})\nabla\Theta(\mathbf{R})\Gamma \\ &\times \int_0^\infty dt e^{-\Gamma t} \frac{\sin(\Delta t)}{\Delta} \\ &= -4\hbar[n_k(2n_2-1)+n_2]G^2(\mathbf{R})\nabla\Theta(\mathbf{R})\Gamma \\ &\times \left[\frac{1}{\Delta^2+\Gamma^2} \right]. \end{aligned} \quad (31)$$

These results are strictly valid at low field intensities. For high intensities, we need to introduce the effects of power broadening. This may be achieved by adding a term in the denominators of Eq. (30) and (31) in such a way that the correct saturation behavior is reproduced [16]. We emphasize that this is fully justified, as will be demonstrated in full optical Bloch equation treatment [14]. Furthermore, we assume that initially the atom is in its ground state, corresponding to setting $n_2=0$. The expression for the reactive force then becomes

$$\langle \bar{\mathbf{F}} \rangle_{\text{react}} = 2\hbar G \nabla G n_k \left[\frac{\Delta}{\Delta^2 + 2n_k G^2 + \Gamma^2} \right] \quad (32)$$

and that of the dissipative force

$$\langle \bar{\mathbf{F}} \rangle_{\text{dissip}} = 2\hbar n_k G^2 \nabla \Theta \left[\frac{\Gamma}{\Delta^2 + 2n_k G^2 + \Gamma^2} \right]. \quad (33)$$

It is the proportionality to Γ in this expression that signifies the dissipative nature of this force and its association with spontaneous emission. Equations (32) and (33) are the main results of this section. In the forms given, these forces are due to a general field distribution. Despite the generality of the results it is possible to draw some conclusions about the characteristics of the forces.

First, it is not difficult to see that, by virtue of its proportionality to Δ and to ∇G , the reactive force would attract the atom to regions of intense field when the laser is tuned below resonance and repel the atom from these regions when tuned above resonance. It is this property of the reactive force that is frequently exploited in atom trapping experiments [17].

The dissipative force, on the other hand, contains the factor $\hbar\nabla\Theta$, which corresponds to the momentum imparted by the light to the atom, which then reradiates spontaneously in a random direction. The probability of spontaneously emitting a photon along a given direction

is the same as that in the opposite direction. The direction of absorption is well defined, so there is a net momentum change per absorbed photon of magnitude $\hbar|\nabla\Theta|$, when averaged over a large number of photons. As the maximum rate at which an atom may spontaneously emit photons is Γ , the maximum dissipative force on the atom is $\hbar\Gamma|\nabla\Theta|$.

Finally, we note that the strength of the reactive force can, to the approximations used, increase without limit as the field intensity, or field gradient, increases. In contrast, the dissipative force is limited to a maximum value, as we have seen. This means that the reactive force would dominate in sufficiently intense fields, as, for example, strong static fields that have significant field gradients and little phase gradient. In the applications discussed in this paper, the typical intensities of the laser light used would render the reactive force negligibly small compared with the dissipative force.

Before proceeding to consider the main application of this paper to the case of atoms and ions in Laguerre-Gaussian beams, it is instructive to consider first the familiar simple case of an atom interacting with a linearly polarized plane wave of wave vector \mathbf{k} and polarization $\hat{\mathbf{e}}_k$ [18]. The expression appropriate for this case is

$$\tilde{\mathcal{E}}(\mathbf{R}) = N\hat{\mathbf{e}}_k e^{i\mathbf{k}\cdot\mathbf{R}}, \quad (34)$$

where N is a normalization factor. Thus we have

$$G(\mathbf{R}) = \frac{N\mathbf{D}_{12}\cdot\hat{\mathbf{e}}_k}{\hbar} \quad (35)$$

and

$$\Theta(\mathbf{R}) = \mathbf{k}\cdot\mathbf{R}. \quad (36)$$

It is then readily shown from Eq. (16) that δ contains the familiar Doppler shift as well as the recoil shift

$$\delta = \mathbf{k}\cdot\mathbf{V} + \frac{\hbar k^2}{2M}, \quad (37)$$

where $\mathbf{V} = \mathbf{P}/M$ is the atomic velocity. The main influence of this effect is to change the detuning parameter from $\Delta_0 = \omega - \omega_0$ to Δ , where $\Delta = \Delta_0 - \delta$. Furthermore, we will ignore the recoil shift on the grounds that it is practically negligible for an atomic mass M and for wave vectors corresponding to visible light, although for low mass and ultracold atoms this may not always be the case [19,20].

The reactive force defined by Eq. (32) for a plane wave is identically zero, which follows trivially from the fact that $\nabla G = 0$. The dissipative force, Eq. (33), on the other hand can be written succinctly in the form

$$\langle \bar{\mathbf{F}} \rangle_{\text{dissip}} = \hbar\mathbf{k}\Gamma \frac{\mathcal{J}}{1 + \mathcal{J} + (\Delta^2/\Gamma^2)}, \quad (38)$$

where \mathcal{J} is a saturation parameter defined by

$$\mathcal{J} = 2n_k G^2 / \Gamma^2. \quad (39)$$

The result (38) agrees with results by other authors [4,5]. In the saturation limit corresponding to $\mathcal{J} \rightarrow \infty$, we obtain the well-known result for the maximum dissipative

force on the atom

$$\langle \vec{\mathbf{F}} \rangle_{\text{dissip}} \approx \hbar \mathbf{k} \Gamma . \quad (40)$$

The dissipative force due to a plane wave produces zero torque on the atom about an axis parallel to the direction of propagation. This property stems from the uniformity of the plane wave, which precludes the presence of nonaxial forces on the atom. In contrast, as we pointed out at the outset and discuss in detail in Sec. III, there exists a class of light beams that are readily reproducible and have nontrivial influence on the nonaxial atomic motion.

III. ATOMS IN LAGUERRE-GAUSSIAN BEAMS

Laguerre-Gaussian modes have recently featured prominently after it was realized that they possess orbital angular momentum [6] about the beam axis. Other forms of light also exhibit this feature, such as the Bessel modes of cylindrical waveguides. The analysis that follows is often simpler for Bessel modes, but it is more useful to consider Laguerre-Gaussian modes as they are readily produced in the laboratory [8]. It should also be recognized that the orbital angular-momentum effects due to intense focused beams may also be possible. It has been shown [21] that appropriate modes possessing orbital angular momentum may exist outside the confines of the paraxial approximation in which the beam aspects of this work have been couched. Within the paraxial approximation [22], we have for a Laguerre-Gaussian beam traveling in the $+z$ direction and polarized principally in the x direction [23]

$$\vec{\mathcal{E}}(\mathbf{R}) = i\omega \left[u_{p,l} \hat{\mathbf{x}} + \frac{i}{k} \frac{\partial u_{p,l}}{\partial x} \hat{\mathbf{z}} \right] e^{ikz} , \quad (41)$$

where the function $u_{p,l}$ may be written in cylindrical coordinates as

$$\begin{aligned} u_{p,l}(r, \phi, z) &= \frac{C}{(1+z^2/z_R^2)^{1/2}} \left[\frac{r\sqrt{2}}{w(x)} \right]^l \\ &\times L_p^l \left[\frac{2r^2}{w^2(z)} \right] e^{-[r^2/w^2(z)]} \\ &\times \exp \left[\frac{ikr^2z}{2(z^2+z_R^2)} \right] e^{il\phi} \\ &\times \exp[i(2p+l+1)\tan^{-1}(z/z_R)] , \end{aligned} \quad (42)$$

where z_R is the Rayleigh range and $w^2(z) = 2(z^2+z_R^2)/kz_R$ is the beam width at distance z from the beam waist. The integer variables l and p are quantum numbers characterizing the mode and C is a normalization factor given in Ref. [8].

A common feature of modes possessing orbital angular momentum is the phase factor $e^{il\phi}$. It is this term that is responsible for the azimuthal Doppler shift and the torque that these beams will be shown to exert on atoms. Another characteristic feature specifically of a Laguerre-Gaussian field distribution is that at any given point the electric-field vector has a component along the beam axis.

For a typical beam this component is small relative to the transverse component. If the atom is isotropic then the atomic dipole can rapidly align with the direction of the local-field polarization. The phase gradient of the z component of the field is the same as that of the x component and so has no impact on the direction of the dissipative force. For these reasons it is sufficient to regard the beam as linearly polarized in the x direction. Once we have made this assumption, we can define functions $G(\mathbf{R})$ and $\Theta(\mathbf{R})$ appropriate for a dipole interacting with a Laguerre-Gaussian mode. We have

$$\begin{aligned} G(\mathbf{R}) &= \omega \frac{\mathcal{C}'}{(1+z^2/z_R^2)^{1/2}} \left[\frac{r\sqrt{2}}{w(x)} \right]^l \\ &\times L_p^l \left[\frac{2r^2}{w^2(z)} \right] e^{-[r^2/w^2(z)]} \end{aligned} \quad (43)$$

and

$$\Theta(\mathbf{R}) = \frac{kr^2z}{2(z^2+z_R^2)} + l\phi + (2p+l+1)\tan^{-1}(z/z_R) + kz . \quad (44)$$

In the above \mathcal{C}' is an overall factor incorporating the appropriate field normalization factor and the dipole matrix element.

The general results of Sec. II can now be used to describe the motion of an atom in a Laguerre-Gaussian beam. Equation (16) enables a direct evaluation of the Doppler shift, which we deal with first, while Eqs. (32) and (33) leads to the forces acting on the atom.

A. Doppler shift

On substituting for the function $\Theta(\mathbf{R})$ using Eq. (44) we straightforwardly obtain from Eq. (16) the Doppler shift δ

$$\begin{aligned} \delta &= \left[\frac{krz}{z^2+z_R^2} \right] V_r + \frac{lV_\phi}{r} \\ &+ \left[\frac{kr^2}{2(z^2+z_R^2)} \left[1 - \frac{2z^2}{z^2+z_R^2} \right] \right. \\ &\quad \left. + \frac{(2p+l+1)z_R}{z^2+z_R^2} + k \right] V_z , \end{aligned} \quad (45)$$

where V_r , V_ϕ , and V_z are the components of the atomic velocity in cylindrical coordinates and the recoil terms have been ignored. The Doppler shift divides naturally into four types of contribution: an axial contribution along the z direction, a contribution due to the Guoy phase, a contribution due to the beam curvature, and finally an azimuthal contribution. We write

$$\delta = \delta_{\text{axial}} + \delta_{\text{Guoy}} + \delta_{\text{curve}} + \delta_{\text{azimuth}} . \quad (46)$$

We now discuss these in turn. The axial component simply corresponds to a Doppler shift that would arise from a plane wave traveling along the beam axis

$$\delta_{\text{axial}} = kV_z . \quad (47)$$

This is normally the dominant shift provided the atom has a substantial velocity component along the beam axis. The shift caused by the Guoy phase is

$$\delta_{\text{Guoy}} = \left[\frac{(2p+l+1)z_R}{z^2+z_R^2} \right] V_z. \quad (48)$$

It is easily seen that, as typically $z_R \gg w_0$, the Guoy shift is very small for practically all Laguerre-Gaussian beams. The shift arising from the beam curvature is given by

$$\delta_{\text{curve}} = \left[\frac{krz}{z^2+z_R^2} \right] V_r + \frac{kr^2}{2(z^2+z_R^2)} \left[1 - \frac{2z^2}{z^2+z_R^2} \right] V_z. \quad (49)$$

This is a sum of contributions due to the spreading of the beam in the radial and axial directions. These contributions are well understood from work on optical cavities. They have the same origin as corresponding shifts in conventional (0,0) mode Gaussian beams [4,17] and arise from the curvature of the wavefront. They may have observable consequences in certain circumstances.

Finally, the azimuthal Doppler shift is

$$\delta_{\text{azimuth}} = \frac{lV_\phi}{r}. \quad (50)$$

The important features of this azimuthal shift are that it is directly proportional to the orbital angular-momentum quantum number l of the Laguerre-Gaussian mode and that it is inversely proportional to the radial atomic coordinate. The shift occurs for motion that is azimuthal to the overall beam propagation.

The azimuthal component in the Doppler shift is just one of the manifestations of the orbital angular-momentum effects of nonuniform beams. As we argue in Secs. IV and V, it is a potentially observable characteristic of the internal motion of the atom arising from its interaction with the LG beam. In the next subsection we consider the radiation forces and an associated torque due to such beams. These, in contrast, are measurable properties of the gross motion of the atom. A different approach to the distinction between internal and gross motion in atoms due to fields possessing orbital angular momentum is that of van Enk and Nienhaus [24].

B. Atom dynamics in LG beams

The dissipative force acting on the atom due to interaction with the Laguerre-Gaussian beam is

$$\langle \tilde{\mathbf{F}} \rangle_{\text{dissip}} = \frac{2\hbar n_k \Gamma}{\Gamma^2 + 2n_k G^2 + \Delta^2} G^2(\mathbf{R}) \nabla \Theta, \quad (51)$$

where $\nabla \Theta$ is obtained in the form

$$\begin{aligned} \nabla \Theta = & \left[\frac{krz}{z^2+z_R^2} \right] \hat{\mathbf{r}} + \frac{l}{r} \hat{\phi} \\ & + \left\{ \frac{kr^2}{2(z^2+z_R^2)} \left[1 - \frac{2z^2}{z^2+z_R^2} \right] \right. \\ & \left. + \frac{(2p+l+1)z_R}{z^2+z_R^2} + k \right\} \hat{\mathbf{z}}. \end{aligned} \quad (52)$$

Note that the Δ appearing in the above expression correctly incorporates the Doppler shift appropriate for a Laguerre-Gaussian beam. We may now introduce a position-dependent saturation parameter $\mathcal{J}(\mathbf{R})$ by

$$\mathcal{J} = \frac{2n_k G^2(\mathbf{R})}{\Gamma^2}. \quad (53)$$

Then the dissipative force takes the form

$$\begin{aligned} \langle \tilde{\mathbf{F}} \rangle_{\text{dissip}} = & \frac{\hbar \Gamma \mathcal{J}}{[1 + \mathcal{J} + \Delta^2/\Gamma^2]} \\ & \times \left\{ \hat{\mathbf{r}} \left[\frac{krz}{z^2+z_R^2} \right] + \hat{\phi} \frac{l}{r} \right. \\ & \left. + \hat{\mathbf{z}} \left[k + \frac{kr^2}{2(z^2+z_R^2)} \left[1 - \frac{2z^2}{z^2+z_R^2} \right] \right. \right. \\ & \left. \left. + \frac{(2p+l+1)z_R}{z^2+z_R^2} \right] \right\}. \end{aligned} \quad (54)$$

This can be written as a sum of four contributions

$$\langle \tilde{\mathbf{F}} \rangle_{\text{dissip}} = \langle \tilde{\mathbf{F}} \rangle_{\text{axial}} + \langle \tilde{\mathbf{F}} \rangle_{\text{azimuth}} + \langle \tilde{\mathbf{F}} \rangle_{\text{curve}} + \langle \tilde{\mathbf{F}} \rangle_{\text{Guoy}}. \quad (55)$$

The first term is a contribution along the axis of the mode

$$\langle \tilde{\mathbf{F}} \rangle_{\text{axial}} = \frac{\hbar \Gamma k \mathcal{J}}{[1 + \mathcal{J} + \Delta^2/\Gamma^2]} \hat{\mathbf{z}} \quad (56)$$

and is seen to be identical to the dissipative force due to a plane wave of wave vector k traveling along the axis. This is the dominant component of the dissipative force. The second, or azimuthal, term is

$$\langle \tilde{\mathbf{F}} \rangle_{\text{azimuth}} = \frac{\hbar \Gamma \mathcal{J}}{[1 + \mathcal{J} + \Delta^2/\Gamma^2]} \left[\frac{l}{r} \right] \hat{\phi}. \quad (57)$$

This force component, whose consequences will be discussed more fully, is seen to be proportional to l/r and acts on the atom in an azimuthal sense. It thus arises principally because of the angular-momentum properties of the LG mode.

The third force component is

$$\begin{aligned} \langle \tilde{\mathbf{F}} \rangle_{\text{curve}} = & \frac{\hbar k \Gamma \mathcal{J}}{[1 + \mathcal{J} + \Delta^2/\Gamma^2]} \\ & \times \left\{ \left[\frac{rz}{z^2+z_R^2} \right] \hat{\mathbf{r}} \right. \\ & \left. + \frac{r^2}{2(z^2+z_R^2)} \left[1 - \frac{2z^2}{z^2+z_R^2} \right] \hat{\mathbf{z}} \right\}. \end{aligned} \quad (58)$$

This has a radial part and an axial part, both of which are attributable to beam curvature. It can be seen that such effects are, in most cases, small in comparison with the axial force. The last force arises from the Guoy phase

$$\langle \tilde{\mathbf{F}} \rangle_{\text{Guoy}} = \frac{\hbar \Gamma \mathcal{J}}{[1 + \mathcal{J} + \Delta^2/\Gamma^2]} \frac{(2p+l+1)z_R}{z^2+z_R^2} \hat{\mathbf{z}}. \quad (59)$$

This force is negligibly small for practically all LG

beams.

Finally, we consider the reactive force as given by Eq. (32). On substituting for G we discover that the reactive force is similar to that for an atom in a (0,0) mode, except that it is sensitive to the particular intensity distribution of the LG beam. Although it has a dependence upon l , it has no azimuthal component. For typical field intensities the reactive force is negligible.

The azimuthal component $\langle \tilde{\mathbf{F}}_{\text{azimuth}} \rangle$ is the only force that is responsible for a torque on the atom about the beam axis. The torque is given by

$$\langle \mathbf{T} \rangle = \langle \mathbf{r} \times \tilde{\mathbf{F}}_{\text{azimuth}} \rangle, \quad (60)$$

where \mathbf{r} is the radial position vector of the atom. We obtain explicitly, using Eq. (57),

$$\langle \mathbf{T} \rangle = l\hbar\Gamma \left[\frac{\mathcal{J}}{[1 + \mathcal{J} + \Delta^2/\Gamma^2]} \right] \hat{\mathbf{z}}. \quad (61)$$

In the saturation limit $\mathcal{J} \rightarrow \infty$ the torque reduces to the simple form

$$\langle \mathbf{T} \rangle \approx l\hbar\Gamma \hat{\mathbf{z}}. \quad (62)$$

The azimuthal force and the torque together with the associated azimuthal Doppler shift are all manifestations of the angular-momentum attributes of the Laguerre-Gaussian beam when it interacts with an atom immersed in it. They constitute the main results of this paper. The effects can be regarded as due to the transfer of $l\hbar$ of angular momentum per scattered photon. The excited atoms spontaneously emit isotropically and consequently the reradiation has no impact on the average momentum, although it will cause fluctuations in the force.

Both the azimuthal shift and the light-induced torque are physically related to the nature of the Poynting vector at any point in the field. At any radius r the vector winds in a helical fashion about the beam axis [6]. Consequently, the Poynting vector is a tangent to a helix. The wave at this point may be regarded as a local plane wave with its wave front normal to the Poynting vector. The azimuthal component of this local plane wave gives rise to both the azimuthal force and its consequent torque, as well as the azimuthal shift in resonance. This is precisely analogous to a plane electromagnetic wave propagating in the z direction, producing a light pressure force proportional to the wave vector \mathbf{k} and to a Doppler shift along the z axis.

IV. ATOMIC TRAJECTORIES AND POSSIBLE EXPERIMENTS

In order to explore the influence of the Laguerre-Gaussian pressure force on atoms and ions we have carried out a simulation program based on the above predictions for the force. The expressions found for the forces are applied to the classical equations of motion for an atom. Essentially, this involves solving Newton's law

$$M \frac{\partial^2 \mathbf{R}(t)}{\partial t^2} = -\nabla U(\mathbf{R}(t)) + \langle \tilde{\mathbf{F}}(\mathbf{R}(t)) \rangle, \quad (63)$$

where only frictional, velocity-dependent, forces are in-

cluded in $\langle \tilde{\mathbf{F}}(\mathbf{R}(t)) \rangle$. We should point out that the classical nature of this law conceals the quantum-mechanically evaluated expectation value of the force as a function of time and position. Solutions of the above equation of motion are sought for three distinct situations corresponding to different forms of the confining potential $U(\mathbf{R})$: (i) when the atom is free as in an atomic beam, (ii) when the atom is trapped in a two-dimensional potential well, and finally (iii) when the atom is trapped in a three-dimensional well, as is appropriate for a Paul trap.

In the simulation we have included only the effects of the dissipative force because the reactive force is practically negligible in the regions of the beam considered. The dissipative force is a position-dependent quantity, so the program had to involve an adiabatic updating of the atomic position, velocity, and force from an initial set of quantities at $t=0$ in small intervals of time up to a final time $t=T_{\text{max}}$. The parameters that are essential for the simulation are chosen as follows.

As our two-level ion we have chosen Mg and the transition $3s^2S_{1/2} \rightarrow 3p^2P_{3/2}$. The Mg atomic mass is $M = 3.98 \times 10^{-26}$ kg and the transition corresponds to a wavelength $\lambda = 280.1$ nm. The choice is influenced by the fact that Mg and this transition have featured in many experiments in laser cooling and trapping [17]. We therefore assume that this is the wavelength $2\pi/k$ of the LG mode. The lifetime of the excited state is $\Gamma = 2.475 \times 10^8 \text{ s}^{-1}$ and for an average laser intensity $I = 10^3 \text{ W m}^{-2}$ this means a Rabi frequency $\Omega \approx \sqrt{10}\Gamma$. The detuning parameter Δ_0 is chosen equal to Γ , that is, $\Delta_0 = \omega - \omega_0 = \Gamma$. The LG beam is characterized by a waist $w_0 = 10^{-5}$ m and a Rayleigh range $z_R = 1.1 \times 10^{-3}$ m. Finally, for illustration, we concentrate on the LG beam characterized by $l=1$.

In Fig. 1 we display the trajectory of a Mg ion irradiat-

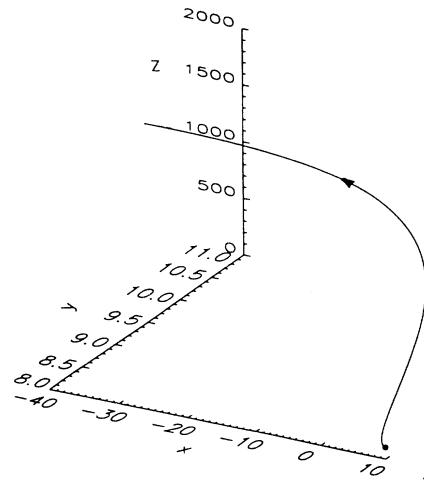


FIG. 1. Trajectory of a free Mg atom with an initial velocity vector $\mathbf{V} = (-0.58, 0, 0) \text{ ms}^{-1}$ in a Laguerre-Gaussian mode with $l=1$, an intensity corresponding to $\Omega/\Gamma = \sqrt{10}$, and detuning $\Delta_0 = \Gamma$. The total time of the trajectory is $T_{\text{max}} = 1.2 \times 10^{-5}$ s. The dot marks the initial position of the atom and the arrow indicates the direction of motion.

ed by an $l=1$ LG beam. The atom is assumed to be initially positioned at the point $\mathbf{R}_0=(8.2, 8.2, 0)$, where distances are measured in units of wavelength λ and the origin of the Cartesian system coincides with the center of the radial LG distribution, conforming to Eq. (42). The initial velocity of the atom is taken to be directed along the negative x axis with a value $v_x(0)=-0.58 \text{ ms}^{-1}$. The figure shows the trajectory from an initial time 0 up to a maximum time $T_{\text{max}}=1.2 \times 10^{-5} \text{ s}$. During this interval the atom is seen to have covered a distance of 2000 wavelengths along the beam axis, but only about 50 wavelengths along x and y . This is a consequence of the dominance of the axial pressure force. However, the twisting due to the azimuthal component of the force is manifest. The influence of the other forces due to the beam curvature and the Guoy phase are too small to lead to any significant changes in this region of the beam, al-

though they have been accommodated, as has the azimuthal Doppler shift.

In Figs. 2(a) and 2(b) a Mg^+ ion irradiated with a LG beam is also subject to a two-dimensional trapping potential, which confines its motion in the x - y plane. We have taken U to have the form

$$U(\mathbf{R}) = \frac{1}{2} M \tilde{\Omega}^2 r^2, \quad (64)$$

where r is the radial coordinate and $\tilde{\Omega}$ is equal to 1.0 MHz. The trajectory shown corresponds to $T_{\text{max}}=1.2 \times 10^{-4} \text{ s}$. It is seen that the ion is influenced by both the axial pressure force and the confining force. The effect of the azimuthal force is apparent in that the atom spirals outwards and appears to approach a constant orbit in the x - y plane. This spiraling out is seen more clearly in Fig. 2(b), which displays a projection of the motion in the x - y plane.

Finally, we have considered confined Mg^+ ions in a Paul trap with U given by

$$U(\mathbf{R}) = \frac{1}{2} M \tilde{\Omega}^2 [r^2 + 4z^2], \quad (65)$$

where $\tilde{\Omega}$ is the same as in Fig. 2 and the total time $T_{\text{max}}=1.2 \times 10^{-4} \text{ s}$. The motion of the ion is rather complicated when seen in three dimensions, as in Fig. 3(a). In Fig. 3(b) we show the projection of the motion in the yz plane and in Fig. 3(c) the projection in the xy plane. Finally, in Fig. 3(d) we display the corresponding projection in the xy plane when the sign of the angular momentum of the LG beam is changed from $l=1$ to -1 . This has the effect of producing a change of the sense of the ionic motion from counterclockwise in Fig. 3(c) to clockwise in Fig. 3(d), as expected. This change in handedness in l is readily achieved experimentally [8].

The results of the simulation presented in Figs. 1–3 immediately suggest the experimental contexts for the observation of the main predictions of this paper. The azimuthal Doppler shift is particularly amenable to experimental measurement for the case of ions in a two-dimensional trap, as illustrated in Fig. 2. It is possible to argue that at any point of the trajectory, the ion can be considered for very short times as being kept in a circular path of radius r with a constant velocity V_ϕ . In this very special case the azimuthal shift can be given a transparent albeit nonrigorous interpretation. The relevant phase factor of the Laguerre-Gaussian mode $e^{il\phi}$ becomes $e^{il(\phi+V_\phi t/r)}$ after time t has elapsed, due to a change in the phase angle by an amount equal to the arc length $V_\phi t$ divided by the radius r . This phase factor yields the azimuthal shift when written in the form $e^{il\phi+il\omega_r t}$ with $\omega_r = V_\phi/r$. In the case of atoms in a Penning trap the velocity V_ϕ is such that ω_r is typically up to a few megahertz. The azimuthal shift is then several megahertz, which is sufficiently large for experimental detection.

It is also reasonable to suggest the detection of the torque using a Paul trap. As we have explained in Fig. 3, ions that are initially at rest in the trap should experience a torque about the axis of the beam causing them to rotate. However, there are ways by which the rotational kinetic energy may be converted into heat and a full

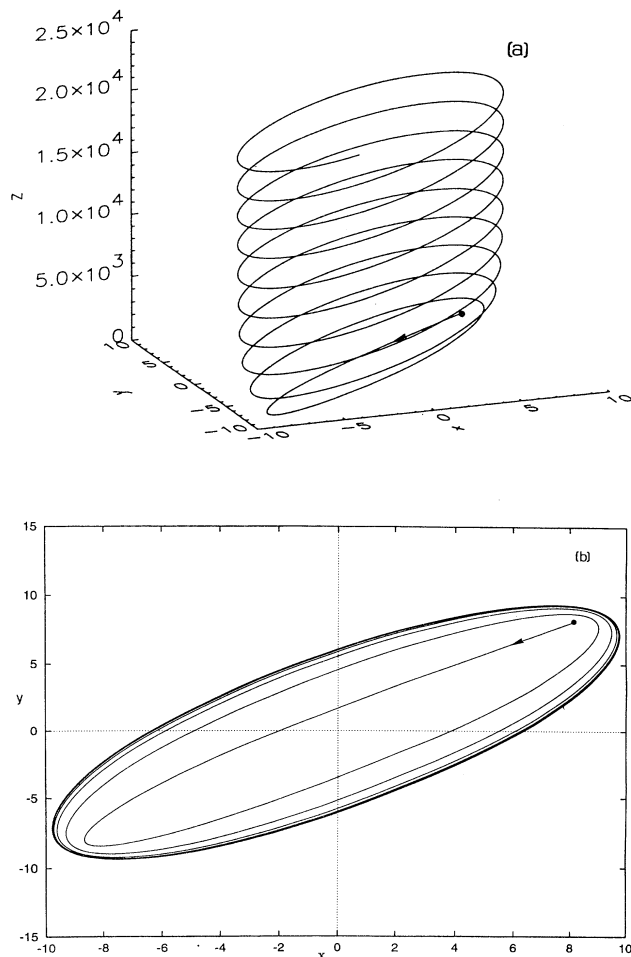


FIG. 2. (a) Trajectory of a Mg^+ ion initially at rest inside a two-dimensional potential. The ion is irradiated with an $l=1$ Laguerre-Gaussian mode and the trajectory time is $T_{\text{max}}=1.2 \times 10^{-4} \text{ s}$. (b) Projection of the trajectory shown onto the x - y plane. Dots mark the initial position of the atom and arrows indicate the direction of motion. All the other parameters are the same as those of Fig. 1.

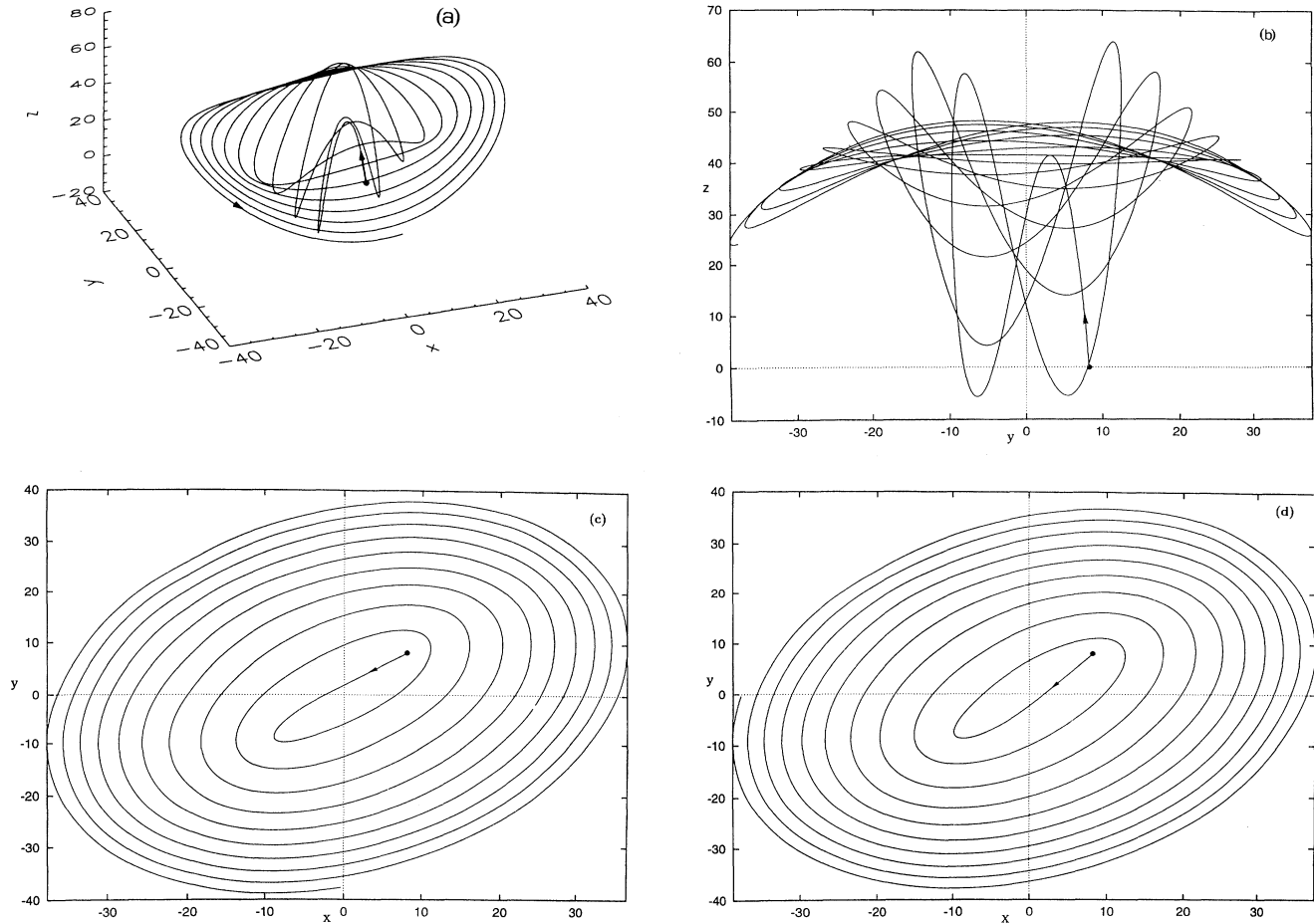


FIG. 3. (a) Trajectory of a Mg^+ ion initially at rest inside a Paul trap. The ion is irradiated by an $l=1$ Laguerre-Gaussian mode; the trajectory time is $T_{\max} = 1.2 \times 10^{-4}$ s and all other parameters are as in Figs. 1 and 2. (b) Projection of the trajectory in the $y-z$ plane. (c) Projection of the trajectory onto the $x-y$ plane. (d) Projection of the trajectory onto the $x-y$ plane corresponding to $l=-1$ for the same T_{\max} and with same parameters. Dots mark the initial position of the atom and arrows indicate the direction of motion.

analysis of the practical limitations of such an experiment needs to be conducted [25]. Other contexts in which the effects of orbital angular momentum are likely to be encountered include crossed-beam experiments and optical molasses, but such situations will not be considered here.

V. COMMENTS AND CONCLUSIONS

The well-defined orbital angular momentum of the photon present in certain kinds of mode can be transferred to atomic systems through resonant interactions. Unusual Doppler shift properties and a torque are found to occur. We have quantified these effects and compared them with effects arising from the interaction of the atom with modes not possessing orbital angular momentum. It is anticipated that the torque should play an important role in interactions between atoms and standing light fields [5], in crossed beams and trapping

experiments. It could indeed play a role in atom interferometry. It appears that these effects should be observable in a variety of atomic experiments. Further theoretical work will include the analysis of radiation pressure using the optical Bloch equations, which will more formally include the effect of spontaneous emission and other relaxation mechanisms [14]. Consideration of the effects of convection currents will become important when specific experiments are considered.

ACKNOWLEDGMENTS

The authors would like to thank R. Loudon and R. C. Thompson for helpful discussions and C. R. Bennett for his help with the computational aspects of this work. Financial support from the EPSRC is acknowledged for W.L.P. and V.E.L. This work was carried out under EPSRC Grant No. GR/J/64009.

- [1] For a succinct historical account see the introduction to the paper by P. Mulser, *J. Opt. Soc. Am. B* **2**, 1814 (1984).
- [2] A. P. Kazantsev, G. I. Surdutovich, and V. P. Yakovlev, *Mechanical Action of Light on Atoms* (World Scientific, Singapore, 1990).
- [3] A. Ashkin, *Phys. Rev. Lett.* **24**, 156 (1970); **25**, 1321 (1970).
- [4] V. G. Minogin and V. S. Letokhov, *Laser Light Pressure on Atoms* (Gordon and Breach, New York, 1986).
- [5] For recent reviews see *Fundamental Systems in Quantum Optics*, Proceedings of the Les Houches Summer School of Theoretical Physics, Session LIII, 1990, edited by J. Dalibard, J.-M. Raimond, and J. Zinn-Justin (Elsevier, Amsterdam, 1992).
- [6] L. Allen, M.W. Beijersbergen, R. J. C. Spreeuw, and J. P. Woerdman, *Phys. Rev. A* **45**, 8185 (1992).
- [7] R. A. Beth, *Phys. Rev.* **50**, 115 (1936).
- [8] M. W. Beijersbergen, L. Allen, H. E. L. O. van der Veen, and J. P. Woerdman, *Opt. Commun.* **96**, 123 (1993).
- [9] M. Babiker, L. Allen, and W. L. Power, *Phys. Rev. Lett.* **73**, 1239 (1994).
- [10] L. Allen, M. Babiker, and W. L. Power, *Opt. Commun.* **112**, 141 (1994).
- [11] M. Babiker, *J. Phys. B* **17**, 4877 (1984).
- [12] M. Wilkens, *Phys. Rev. A* **49**, 570 (1994).
- [13] V. E. Lembessis, M. Babiker, C. Baxter, and R. Loudon, *Phys. Rev. A* **48**, 1594 (1993).
- [14] L. Allen, M. Babiker, and V. E. Lembessis (unpublished).
- [15] R. H. Dicke and J. P. Wittke, *Introduction to Quantum Mechanics* (McGraw-Hill, New York, 1966), p. 274.
- [16] L. Allen and J. Eberly, *Optical Resonance and Two-level Atoms* (Dover, New York, 1987).
- [17] P. E. Toschek, in Proceedings of the Les Houches Summer School of Theoretical Physics, Session XXXVIII, 1982, edited by G. Grynberg and R. Roston (Elsevier, Amsterdam, 1984), p. 381.
- [18] We assume throughout that axial field propagation is in the $+z$ direction, in contrast to the opposite sense adopted in Refs. [9] and [10].
- [19] S. J. van Enk, *Quantum Opt.* **6**, 445 (1994).
- [20] K. M. Gheri, H. Ritsch, D. F. Walls, and V. I. Balykin, *Phys. Rev. Lett.* **74**, 678 (1995).
- [21] S. M. Barnett and L. Allen, *Opt. Commun.* **110**, 670 (1994).
- [22] A. E. Siegman, *An Introduction to Lasers and Masers* (McGraw-Hill, New York, 1971).
- [23] H. A. Haus, *Waves and Fields in Optoelectronics* (Prentice Hall, Englewood Cliffs, NJ, 1984).
- [24] S. J. van Enk and G. Nienhaus, *J. Mod. Opt.* **41**, 963 (1994).
- [25] W. L. Power and R. C. Thompson (unpublished).